Commun. Comput. Phys.
doi: 10.4208/cicp.300911.090312a

Vol. **13**, No. 2, pp. 526-539
February 2013

Investigation of Possible Half-Metallic Antiferromagnets on Double Perovskites $A_2BB'O_6$ (A=Ca, Sr Ba; B,B'=Transition Metal Elements)

S. H. Chen[1,*], Z. R. Xiao[2], Y. P. Liu[3] and Y. K. Wang[4,*]

[1] *Institute of Physics, Academia Sinica, Taipei 11529, Taiwan.*
[2] *Graduate Institute of Applied Physics, National Chengchi University, Taipei 11605, Taiwan.*
[3] *Department of Physics, National Taiwan Normal University, Taipei 106, Taiwan.*
[4] *Center for General Education and Department of Physics, National Taiwan Normal University, Taipei 106, Taiwan.*

Received 30 September 2011; Accepted (in revised version) 9 March 2012

Communicated by Michel A. Van Hove

Available online 17 July 2012

Abstract. A search was made for possible half-metallic (HM) antiferromagnet (AFM) in all the (C_2^{29}=406) double perovskites structures of $Sr_2BB'O_6$ where BB' pairs are any combination of 3d, 4d or 5d transition elements with the exception of La. Sr can also be replaced by Ca or Ba whenever HM-AFM was found and similar calculations were then performed in order to probe further possibilities. It was found that A_2MoOsO_6, A_2TcReO_6, A_2CrRuO_6, where A=Ca, Sr, Ba, are all potential candidates for HM-AFM. The AFM of $A_2BB'O_6$ comes from both the superexchange mechanism and the generalized double exchange mechanism via the $B(t_{2g})$-O2p_π-$B'(t_{2g})$ coupling, With the latter also being the origin of their HM. Also considered were the effects of spin-orbit coupling (SOC) and correlation (+U) by introducing +SOC and +U corrections. It is found that the SOC effect has much less influence than the correlation effect on the HM property of the compounds. For A_2TcReO_6 and A_2CrRuO_6, after +U, they become nearly Mott-Insulators. In the future, it is hoped that there will be further experimental confirmation for these possible HM-AFM candidates.

PACS: 75.10.Lp, 71.20.-b, 75.30.-m, 75.50.Ee

Key words: Half-metal antiferromagnet, GGA +U, superexchange, generalized double exchange.

*Corresponding author. *Email addresses:* chen_shao_hua197@yahoo.com.tw (S. H. Chen), zrxiao@gmail.com (Z. R. Xiao), viva.guitarra@gmail.com (Y. P. Liu), kant@ntnu.edu.tw (Y. K. Wang)

1 Introduction

The characteristic properties of half-metallic (HM) materials are spin magnetic moments quantized with a fully spin-polarized state at the Fermi level, as well as zero spin susceptibility. In 1983, R. de Groot et al. [1] discovered HM ferromagnets (FM) by calculating the band structure of the magnetic semi-Heusler compounds NiReSb and PtReSb. Due to their single-spin charge carriers, HM materials can be applied as single-spin electron sources and high-efficiency magnetic sensors [2–11]. If the total magnetic moment is zero in HM material, it is called HM antiferromagnet (AFM). The first HM-AFM was proposed by van Leuken and de Groot [12] in 1995. HM-AFMs have the following properties: First, they do not carry any macroscopic magnetic field in zero temperature, even thought small magnetization might be induced due to finite temperature spin fluctuations [13]. Second, they can transport a 100% spin polarized charge without net magnetization. Third, theirs magnetic susceptibility is zero. Based on these features, HM-AFMs have several applications: they can be used as probes in spin-polarized scanning tunneling microscopes since they will not disturb the spin character of the sample; as well they play an important role in spintronic devices. However, up till now, there still exists no experimental verification for them.

Many structures are considered as possible HM-AFM candidates, e.g. half-Heusler [12], full-Heusler alloys [14–17], thiospinels [18], Fe-based superconductor [19] and superlattices [20, 21]. They can also be found in some disorder systems, e.g. vacancy-induced rock salt transition metal oxides [23], Co-substituted Heusler alloys [24], and diluted antiferromagnetic (AFM) semiconductors [25, 26]. Pickett [27] first looked for HM-AFMs using the (fixed) cubic double perovskite structure $La_2M'M''O_6$ in 1998. He proposed La_2VMnO_6 and La_2VCuO_6 as two promising candidates for HM-AFM. He also mentioned that the perovskite crystal structure AMO_3, due to its simple crystal structure, potentially large number of members, and strong coupling between magnetic ordering and electronic properties, appeared to be an ideal system in the search for HM-AFM members.

Based on a systematic first-principle study of the ordered double perovskites $A_2BB'O_6$, whose nominal ionic picture is $A_2^{2+}(BB')^{8+}O_6^{2-}$, with possible B and B' pairs in the $3d$, $4d$ and $5d$ transition metal elements. We predict A_2CrRuO_6, A_2MoOsO_6 and A_2TcReO_6 as possible HM-AFM candidates. Among them, only Sr_2CrRuO_6 was previously predicted by Lee and Pickett [32]. We considered two stacked structures ([111], space group $Fm\bar{3}m$, and [001], space group $P4/mmm$, as seen in Fig. 1) with two magnetic states (FM and nonconventional AF (labeled as AF-I), whose spin moment of (B, B, B', B') is (+,+,−,−,)). Furthermore, we also considered the possibilities of a third magnetic states: conventional AF (labeled as AF-II, whose spin moment of (B, B, B', B') is (+,−,+,−,)), which has seldom been compared with AF-I in term of stability in theoretical predictions of HM-AFMs in double perovskites structures.

For transition metal oxides, we took into account spin-orbit coupling (SOC) and correlation ($+U$) effects. The Hubbard U values for all transition metals are reported [33]

and we take U values from minimum to maximum in our calculations. Under $+U$ and SOC corrections, calculations show that HM characteristics are enhanced in A_2MoOsO$_6$ and quenched in both A_2TcReO$_6$ and A_2CrRuO$_6$.

2 Crystal structure and calculation methods

There are two types of ordered double perovskites structure $A_2BB'O_6$ (A = Ca, Sr, Ba). One is a [111] stacked structure ($Fm\bar{3}m$ space group, Fig. 1(a)), in which B and B' layers are stacked along the [111] direction, the other a [001] stacked structure ($P4/mmm$ space group, Fig. 1(b)). Detailed descriptions of these two stacked structures can be found in Ref. [24]. As well, there exist two types of AFM states. The first we label as an AF-I state in which B and B' ions are antiferromagnetically polarized. Material within this state could has possibility to be a HM, (i.e. a HM-AFM) since the bands of B and B' ions are usually different from each other. The second type of AFM (conventional AFM) we label as an AF-II state in which B and B' ions along the chain are antiferromagnetically polarized but neighboring chains are antiferromagnetically coupled. (i.e. (B, B, B', B') is (+,−,+,−,) in superlattice, as seen in Fig. 2.) The total density of state (DOS) of spin-up and spin-down is symmetric, resulting from the induced equivalence in the charges: Q↑[B (B')] = Q↓[B (B')]. Due to its symmetrical DOS, material within this conventional AFM state (such as bcc Cr) has no chance to be a HM. After full structural optimization, $Fm\bar{3}m$ becomes $I4/mmm$ space group in the FM and AF-I states in [111] stacked structure, while $P4/mmm$ remains unchanged in the AF-II state in both stacked structures but reduced to the $P4/mm$ space group in FM and AF-I states in [001] stacked structure.

Our calculations were based on density functional theory (DFT) with both GGA and GGA $+U$ approaches, where $+U$ is on-site Coulomb interaction correction. The crystal shapes and ionic positions were fully optimized using full-potential projector augmented wave (PAW) method [34] within conjugate-gradient (CG) method implemented in VASP code [35]. The Brillouin zone were sampled with a $8\times8\times6$ Monkhorst-Pack grid (30 k-points in the irreducible Brillouin zone wedge). A cutoff energy of 450 eV was set for plane waves. Theoretical equilibrium structures were obtained when the forces and stresses acting on all the atoms were less than 0.02 eV/A and 1.0 kBar, respectively. Next, we used the WIEN2k package [36] with the all electron full-potential linearized augmented plane wave (FLAPW) method [37,38] for calculating the electronic structures and magnetic properties. A cutoff angular momentum ($L_{\max}$) of 10 for the wave function and of 6 for the charge density / potential. The number of augmented plane waves was about 115 per atom, i.e. $R_{mt}\cdot K_{\max}=6$ (the total energies are converged, since their difference from that of $R_{mt}\cdot K_{\max}=7$ are within 3%). The improved tetrahedron method was used for the Brillouin zone integration [39]. 120, 159, 84 and 30 k-points numbers were used in the irreducible Brillouin zone wedge for the $Fm\bar{3}m$, $I4/mmm$, $P4/mmm$ and $P4/mm$ structures, respectively (the total energies are converged, since their difference from that of double k-points are within 10%). The muffin-tin sphere radii were set to 2.5

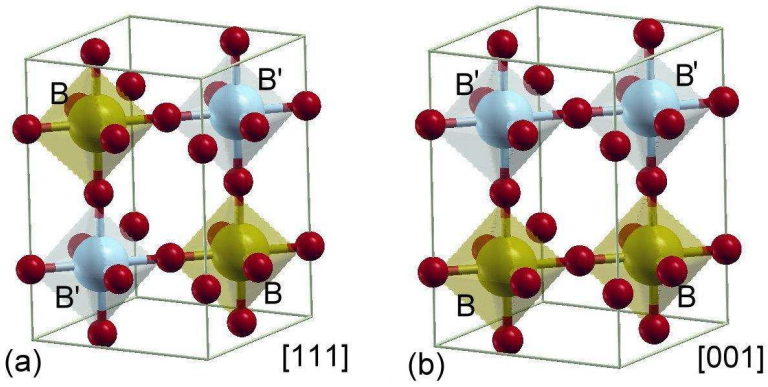

Figure 1: (Color online) (a) Cubic $Fm\bar{3}m$ [111] and (b) tetragonal $P4/mmm$ [001] stacked structure.

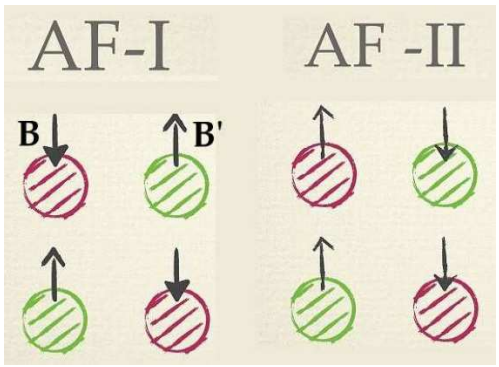

Figure 2: (Color online) Two type of AFM states, we label as AF-I/AF-II in which the spin state of (B, B, B', B') is (+,+,−,−,)/(+,−,+,−,).

a.u. for Ca, Sr, Ba; and 2.0 a.u. for Cr, Ru, Mo, Os, Tc, Re; and 1.4 a.u. for O. Strong correlation effects were set by GGA +U calculation [40, 41], including on-site U (2, 4 eV for Ru, Mo, Os, Tc, Re, and 3, 6 eV for Cr) and J (0.87 eV) [31, 33, 42] for d orbitals of Cr, Ru, Mo, Os, Tc and Re.

3 Results and discussions

3.1 HM-AFMs from the initial search and stable phase

The chemical formula $A_2BB'O_6$, BB' can be any pair taken from the 29 transition metal elements except La. This means there are 406 (C_2^{29}) combinations of possible compounds here. This is a time-consuming task. In searching for HM-AFMs, we first used FLAPW method to calculate the self-consistent electronic structure of all 406 $Sr_2BB'O_6$ compounds

in the ideal cubic $Fm\bar{3}m$ structure with fixed lattice constant a $\sim$ 7.90 $\AA$ in a AF-I state. We found five BB' pairs which could be HM-AFMs $Sr_2BB'O_6$ compounds, namely, VIr, CrRu, NiOs, MoOs, and TcRe. Out of these, only CrRu was previously predicted by Lee and Pickett [32]. Following, we performed structural optimizations with both the initial states of FM and AF-I and found that the total energy of the AF-I state in Sr_2NiOsO_6 was higher than that of the FM state by 0.182 eV/f.u. and Sr_2VIrO_6 had become a nonmagnetic state. This suggests that the HM-AFM state is not stable in these two compounds and, therefore, they will not be considered further.

In order to find the stable magnetic phase and structure in these three newly found compounds-Sr_2CrRuO_6, Sr_2MoOsO_6, and Sr_2TcReO_6-we performed electronic structure calculations of FM, AF-I and AF-II phases in both [111] and [001] structures. We also replaced Sr in these compounds with Ca or Ba and then did the same calculations. To guarantee the accuracy of the calculation results, a full structural optimization with higher convergence criteria was performed. The calculated total energy of A_2CrRuO_6, A_2MoOsO_6, and A_2TcReO_6 for the [111] stacked structure in a AF-I state was around 9.8, 11.5 and 1.3 eV/f.u., respectively; lower than that of the [001] stacked structure. It shows a huge energy difference between the [111] stacked and [001] stacked structure and indicates that the [111] stacked structure is more stable; and thus, we will not consider the [001] stacked structure further. Corresponding all ordered double perovskites structures $A_2BB'O_6$ (A = Ca, Sr, Ba) discussed later in this paper are [111] stacked structures.

Comparison of energy in [111] stacked structures:

(1) For A_2MoOsO_6, the initial FM and AF-I states all converge to an AF-I state where A = Ca, Sr. The AF-II state of Ca_2MoOsO_6 and Sr_2MoOsO_6 are higher than that of the AF-I state by only 0.010 and 0.008 eV/f.u., respectively. However, the FM, AF-I and F-II states of Ba_2MoOsO_6 all converge to the NM state.

(2) For A_2TcReO_6, the initial FM state converges to a NM state. The AF-II state of Ca_2TcReO_6, Sr_2TcReO_6, and Ba_2TcReO_6, are higher than that of the AF-I state, here by 0.168, 0.183, and 0.234 eV/f.u., respectively. The total energy of the AF-I state is lower than the FM/NM and AF-II state is HM, and is the most stable.

(3) For A_2CrRuO_6, we find that the initial FM and AF-I states all converge to a AF-I state. The AF-II state of Ca_2CrRuO_6, Sr_2CrRuO_6, and Ba_2CrRuO_6 is higher than that of the AF-I state by 0.159, 0.377, and 0.352 eV/f.u., respectively. Again, the AF-I state is HM and the most stable.

In conclusion, the AF-I state in the [111] stacked structure is the most stable state in $A_2BB'O_6$ (A = Ca, Sr, Ba, BB'= CrRu, MoOs and TcRe). We list their calculated structural parameters in a fully optimized $I4/mmm$ structure in Table 1. The lattice constant a grows larger as the size of atom A gets larger. There are two O_1 atoms sitting above and below the B and B' atoms along the Z axis, and four other O_2 atoms sitting on the same plane as the B and B' atoms. Their c/a ratio is very close to the ideal value of $\sqrt{2}$, meaning that their structural shape is very close to an ideal double perovskites structure

Table 1: Calculated structural parameters of the AF-I $A_2BB'O_6$ in the fully optimized $I4/mmm$ [111] structure, which B (0, 0, 0), B' (0, 0, $\frac{1}{2}$) and A (0, $\frac{1}{2}$, $\frac{1}{4}$).

BB'	MoOs			TcRe			CrRu		
A	Ca	Sr	Ba	Ca	Sr	Ba	Ca	Sr	Ba
a (Å)	5.5851	5.6456	5.7459	5.5885	5.6518	5.7534	5.4450	5.5251	5.6564
c/a	1.4147	1.4146	1.4150	1.4143	1.4145	1.4147	1.4142	1.4138	1.4140
V (Å^3/f.u.)	123.23	127.27	134.22	123.42	127.68	134.72	114.15	119.23	127.95
O_1 x	0	0	0	0	0	0	0	0	0
y	0	0	0	0	0	0	0	0	0
z	0.2484	0.2477	0.2464	0.2519	0.2521	0.2528	0.2462	0.2467	0.2477
O_2 x	0.2516	0.2523	0.2536	0.2482	0.2480	0.2472	0.2538	0.2533	0.2522
y	0.2516	0.2523	0.2536	0.2482	0.2480	0.2472	0.2538	0.2533	0.2522
z	0.5	0.5	0.5	0.5	0.5	0.5	0.5	0.5	0.5

($Fm\bar{3}m$ space group). It also means that their BO_6, $B'O_6$ are both approximately right octahedrons. For example, in Sr_2TcReO_6, the Re-O_1 bond length is 1.9822$\mathring{A}$ (z direction), and the Re-O_2 bond length is 1.9823$\mathring{A}$ (xy plane), can be regard as "identical, within numerical precision." See also the Tc-O_1 bond length is 2.0150$\mathring{A}$ (z direction) and the Tc-O_2 bond length is 2.0141$\mathring{A}$ (xy plane), nearly the same as the former. The angle of the B-O-B' bond remains 180°.

3.2 Electronic structure and magnetic properties

The nominal ionic picture of $A_2BB'O_6$ is $A_2^{2+}(BB')^{8+}O_6^{2-}$. For example, in Sr_2MoOsO_6, the transition metal atoms Mo and Os have a nominal valence configuration of $Mo^{4+}(4d^2)$ and $Os^{4+}(5d^4)$, respectively. The AFM coupling of $Mo^{4+}(t_{2g}^2\downarrow, S=-1)$ and $Os^{4+}(t_{2g}^3\uparrow t_{2g}^1\downarrow, S=1)$, which exists in a low spin state (see Fig. 3), results in zero total magnetic moment. This is an AFM state. For Sr_2TcReO_6, the transition metal atoms Tc and Re have a nominal valence configuration of $Tc^{4+}(4d^3)$ and $Re^{4+}(5d^3)$, respectively. For Sr_2CrRuO_6, the transition metal atoms Cr and Ru have a nominal valence configurations of $Cr^{4+}(3d^2)$ and $Ru^{4+}(4d^4)$, respectively.

We list the calculated physical properties of $A_2BB'O_6$ in a fully optimized $I4/mmm$ structure in Table 2. The results of GGA + SOC, GGA +U and GGA + SOC +U calculations are in brackets. The corresponding total and orbital-decomposed DOS are displayed in Figs. 3-7. For Ca_2MoOsO_6 and Sr_2MoOsO_6 (as seen in Fig. 3) we observe that the Mo, Os have only spin-down electrons at the Fermi level. The lower valence band consist mainly of O $2p$ electrons, while the spin-up Os t_{2g} dominates the upper valence band. The Mo and Os d orbitals contribute to the lower valence band as a result of hybridization between O_{2p} and Mo (Os) d orbitals. The octahedron crystal field causes the Mo (Os) e_g dominant band to be higher than the Mo (Os) t_{2g} dominant band. However, one can see that the spin-up gap $E_{g\uparrow}$ of Ba_2MoOsO_6 disappears under structural optimization. In Ta-

Table 2: Calculated physical properties of the AF-I state $A_2BB'O_6$ in the fully optimized $I4/mmm$ [111] structure. The unit of $N(E_F)$ is (states/eV/f.u.).

A=	Ca	Sr	Ba
Method		GGA(+SOC/+U/+U+SOC)	
		A_2MoOsO$_6$	
m_{Mo} (μ_B)	-0.38 (-0.33/0.77/0.72)	-0.30 (-0.21/-0.74/-0.68)	0.00 (0.00/0.61/0.55)
m_{Os} (μ_B)	0.36 (0.25/-0.72/-0.61)	0.28 (0.15/0.69/0.57)	0.00 (0.00/-0.56/-0.45)
m_t (μ_B)	0.00 (-0.09/0.00/0.08)	0.00 (-0.08/0.00/-0.08)	0.00 (0.00/0.00/0.07)
$N(E_F)\uparrow$	0.00 (0.56/0.00/0.11)	0.00 (0.72/0.00/0.13)	1.03 (1.10/0.00/0.18)
$N(E_F)\downarrow$	2.97 (2.86/2.92/2.93)	2.99 (2.55/3.10/3.09)	1.03 (1.10/3.38/3.19)
$E_{g\uparrow}$ (eV)	0.12 (0.00/0.94/0.68)	0.10 (0.00/0.95/0.68)	0.00 (0.00/0.84/0.44)
		A_2TcReO$_6$	
m_{Tc} (μ_B)	-1.31 (-1.31/-1.59/-1.57)	-1.34 (-1.33/-1.60/-1.57)	-1.34 (-1.32/-1.58/-1.56)
m_{Re} (μ_B)	1.16 (1.10/1.42/1.36)	1.19 (1.12/1.42/1.36)	1.18 (1.11/1.41/1.35)
m_t (μ_B)	0.00 (-0.09/0.00/-0.06)	0.00 (-0.09/0.00/-0.07)	0.00 (-0.1/0.00/-0.07)
$N(E_F)\uparrow$	1.92 (1.69/0.10/0.09)	1.45 (1.27/0.17/0.06)	1.09 (1.08/0.12/0.08)
$N(E_F)\downarrow$	0.00 (0.00/0.00/0.00)	0.00 (0.00/0.00/0.00)	0.00 (0.00/0.00/0.00)
$E_{g\downarrow}$ (eV)	0.74 (0.50/1.61/1.22)	0.87 (0.60/1.70/1.43)	0.95 (0.66/1.65/1.44)
		A_2CrRuO$_6$	
m_{Cr} (μ_B)	-1.96 (-1.95/-2.29/-2.27)	-2.01 (-2.01/-2.33/-2.31)	-2.10 (-2.09/-2.39/-2.37)
m_{Ru} (μ_B)	1.38 (1.37/1.61/1.58)	1.39 (1.38/1.60/1.58)	1.39 (1.38/1.58/1.55)
m_t (μ_B)	0.00 (0.00/0.00/0.00)	0.00 (0.00/0.00/0.00)	0.00 (0.00/0.00/0.00)
$N(E_F)\uparrow$	0.00 (0.00/0.00/0.00)	0.00 (0.00/0.00/0.00)	0.00 (0.00/0.00/0.00)
$N(E_F)\downarrow$	2.47 (2.71/0.11/0.03)	1.75 (1.95/0.44/0.05)	0.29 (0.29/1.38/0.85)
$E_{g\uparrow}$ (eV)	1.00 (1.62/1.67/1.66)	0.93 (0.92/1.58/1.54)	0.87 (0.76/1.42/1.40)

ble 1, one can see that the quantity of change of O_1 and O_2 from the ideal positions (O_1(0, 0, 0.25), O_2(0.25, 0.25, 0.5)), is rather larger in Ba_2MoOsO_6. Because of the distortions of MoO_6 and OsO_6 octahedron, the change in the crystal field shifts the Mo, Os t_{2g} bands and the HM characteristic disappears. These changes in the HM and AF-I as a result of the effect of structural optimization is explained in Ref. [22] using $LaSrVRuO_6$ as an example. Briefly speaking, the weakness of the AF-I and FM state in Ba_2MoOsO_6 found in the ideal $Fm\bar{3}m$ structure were unable to sustain such structural distortions and, as a result, both of them become nonmagnetic.

For A_2TcReO_6, as shown in Fig. 4, its DOS property is similar to that of Sr_2MoOsO_6, which has been discussed above, except that we have chosen Tc atoms to be negative spin moments in the spin-down channel and Re as the positive channel. However, the hybridization between Tc and Re on the Fermi level is relatively weak. In fact, the interaction between Tc and Re can be considered as superexchange mechanism because of their half-filled of t_{2g} orbitals. Even though the band gaps E_g are obviously larger than that

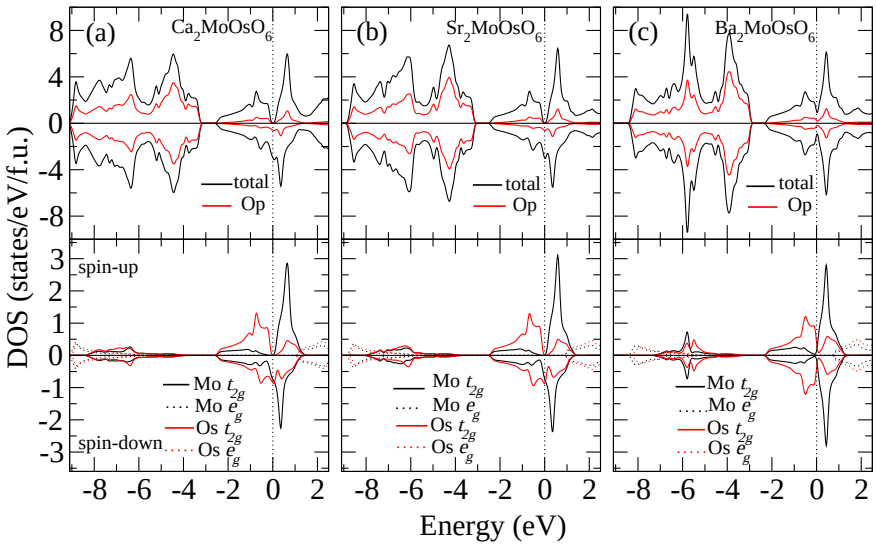

Figure 3: Total and orbital-decomposed density of states of A_2MoOsO$_6$ (A=Ca, Sr, Ba) with $I4/mmm$ [111] structure by GGA calculations.

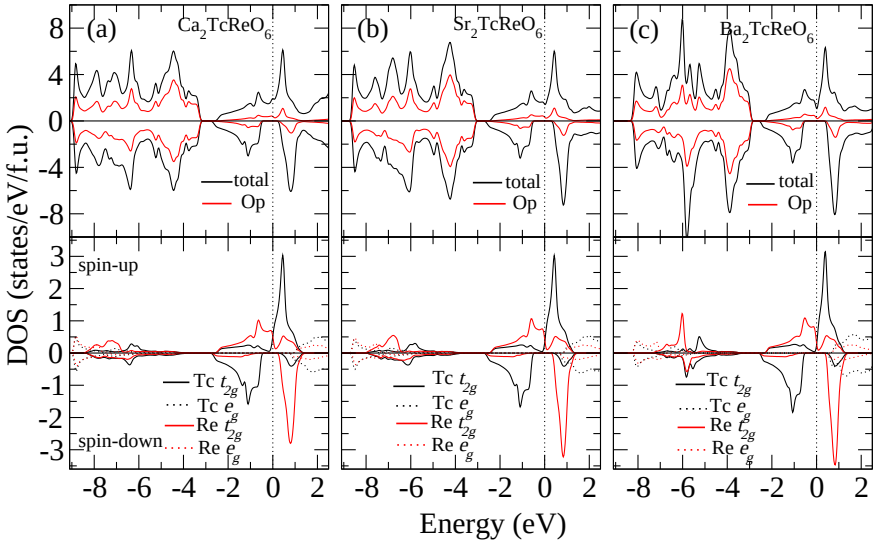

Figure 4: Total and orbital-decomposed density of states of A_2TcReO$_6$ (A=Ca, Sr, Ba) with $I4/mmm$ [111] structure by GGA calculations.

in A$_2$MoOsO$_6$, but superexchange shows no help to hopping Tc and Re near the Fermi level.

For Sr$_2$CrRuO$_6$ in Fig. 5, its DOS is similar to that in Lee and Pickett's work [32] except for the opposite spin state. There is a small dip or pseudogap at E_F in the spin-down channel of Ba$_2$CrRuO$_6$, which may be regarded as a semimetal with a small DOS of 0.29 states/eV/f.u. at E_F.

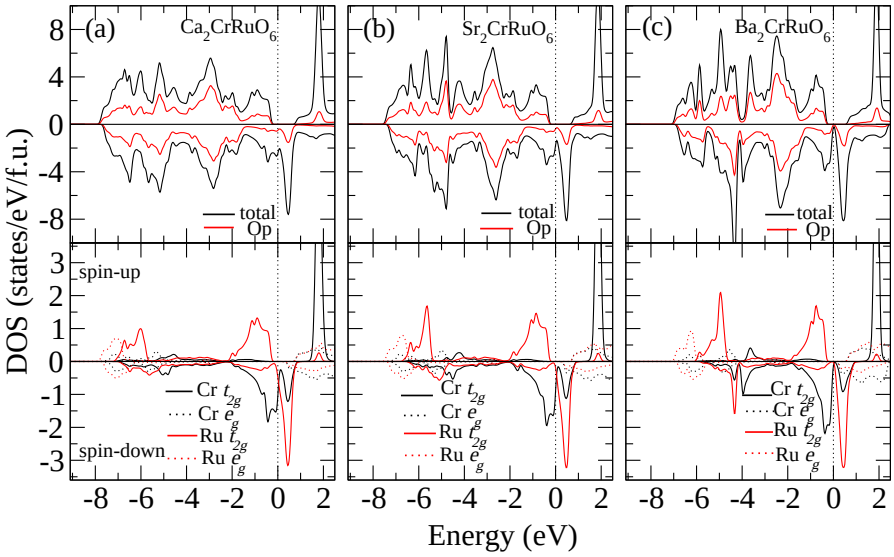

Figure 5: Total and orbital-decomposed density of states of A_2CrRuO$_6$ (A=Ca, Sr, Ba) with $I4/mmm$ [111] structure by GGA calculations.

The HM of $A_2BB'O_6$ is essentially similar to that of HM ferrimagnetic double perovskites, such as Sr_2FeMoO_6 [46, 47]. For example, the on-site exchange lowers the majority spin Os t_{2g} band below E_F and pushes the minority spin Mo t_{2g} band above E_F, resulting in an insulating gap amid the spin-up channel. Accordingly, the band gap in Sr_2MoOsO_6 may be called an antiferromagnetic coupling gap. The AFM of $A_2BB'O_6$ comes from both the superexchange coupling of B d-O p-B' d σ-bonding and the double exchange coupling of $B(t_{2g})$-O2p-$B'(t_{2g})$ π-bonding. The former is similar to the conventional superexchange in the AFM insulators (e.g. NiO); the later, which has been called a generalized double exchange mechanism [44, 45], is similar to the double exchange mechanism of metallic ferromagnetism in colossal magnetoresistive magnets [43]. This non-local indirect exchange interaction enhances the AFM exchange coupling of B and B' ions. For further information, there are detailed discussions concerning these two exchange couplings in our two previous papers of 2006 [28] and 2009 [30].

3.3 Correlation and spin-orbital coupling effects

In consideration of the electron-electron strong correlation effect in transition metal oxides, GGA +U calculations [40] are used to correct this effect [41]. In this research, we imposed U = 2.0 eV [42] and J = 0.87 eV [22] on d orbitals of Ru, Mo, Os, Tc and Re and U = 3.0 eV on the d orbitals of Cr. We have also done calculations for larger U (e.g. U = 4 eV for Mo, Os, Tc, Re, Ru and U = 6 eV for Cr), and the qualitative behaviors of the systems are identical with that in smaller U. For the reason of the space of printed pages, we just put one of these results on the paper. These U, J values are chosen in reasonable

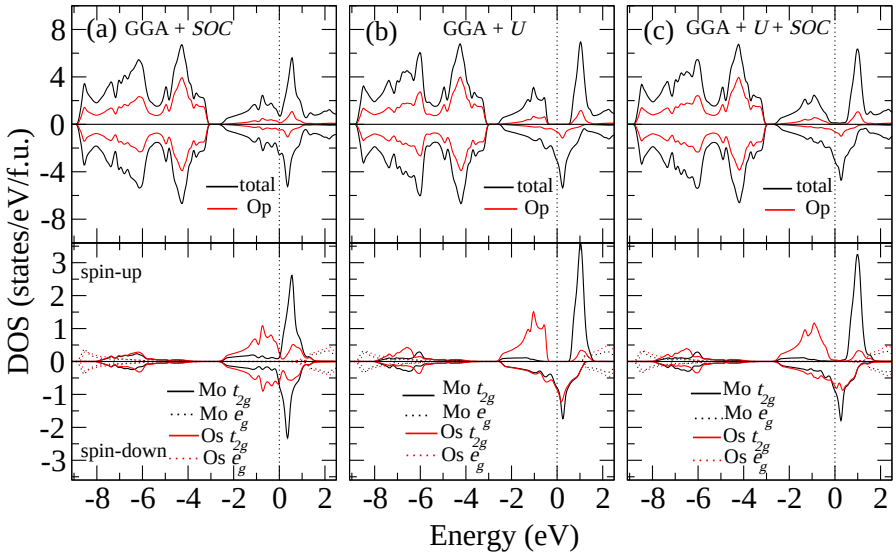

Figure 6: Total and orbital-decomposed density of states of Sr_2MoOsO_6 with $I4/mmm$ [111] structure, which $U = 2$ eV for Mo and Os, and spin-orbital coupling (SOC).

range for qualitatively looking for possible HM-AFM candidates. The exact values of U and J of the compounds need more specified method to find out, or maybe one can do X-ray emission spectra (XES) experiments to compare to our results (DOS of GGA and GGA+U). It was found that the correlation effect ($+U$) enhanced the local magnetic moments of Cr, Ru, Mo, Os, Tc and Re. For example, in Sr_2MoOsO_6 without $+U$ (Table 2), the local magnetic moments m_{Mo} and m_{Os} are -0.301 μ_B and 0.278 μ_B, respectively. However, with $+U$, m_{Mo} becomes -0.744 μ_B and m_{Os} increases to 0.685 μ_B.

Since the DOS of A_2MoOsO_6 (A_2TcReO_6 and A_2CrRuO_6) with +SOC/$+U$/$+U$+SOC is similar with each Ca, Sr or Ba, we merely show Sr_2MoOsO_6, Sr_2TcReO_6 and Sr_2CrRuO_6. On one hand, $+U$ enlarges the energy difference between spin-up and spin-down d-electrons, i.e. it raises the Mo $t_{2g\uparrow}$ and $e_{g\uparrow}$ bands and lowers the Os $t_{2g\uparrow}$ band with respect to the Fermi-level (see Fig. 6(b)). Therefore, a gap on the spin-up channel ($E_{g\uparrow}$) has once again been opened and a HM state is present in Ba_2MoOsO_6. On the other hand, compared to the DOS of Sr_2MoOsO_6 (see Fig. 3), we can see that the peak of Os $t_{2g\downarrow}$ band is shifted upward (Fig. 6(b)) and the $N_{t_{2g\downarrow}}(E_F)$ is larger than that without $+U$. As a result, the double exchange between Mo and Os $t_{2g\downarrow}$ electrons is enhanced, or in other words, the AFM coupling between Mo and Os is enhanced. In Ba_2MoOsO_6, $+U$ enhances (corrects) the spin-polarization (local magnetic moment) of Mo and Os so that the AFM coupling between Mo and Os can sustain the structural distortions and remain a HM-AFM state. The reason being that following the $+U$ correction (on-site Coulomb repulsion) is larger than the energy band widening from the structural distortions. The bands are separated. The bands shifting downward have more electrons and those shifting upward have less electrons, such that maintain higher spin moments, thereby restor-

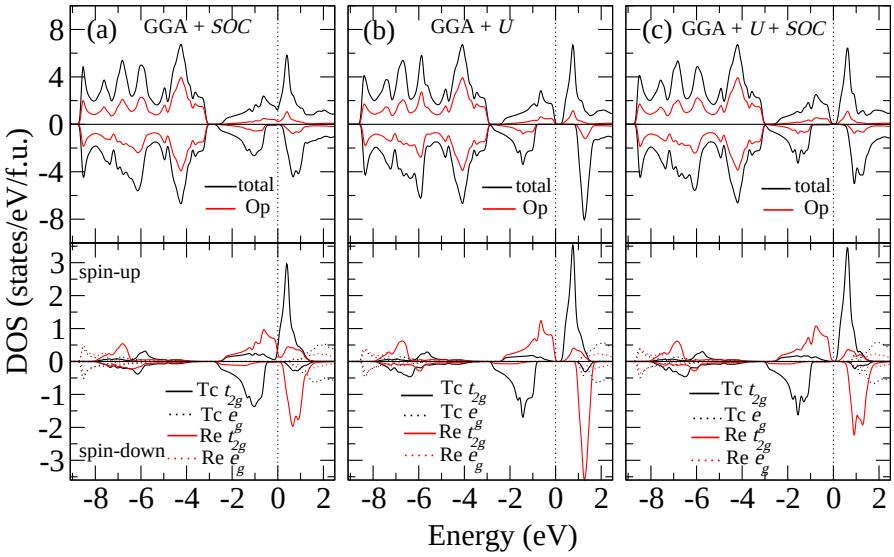

Figure 7: Total and orbital-decomposed density of states of Sr_2TcReO_6 with $I4/mmm$ [111] structure, which $U = 2$ eV for Tc and Re, and including spin-orbital coupling (SOC).

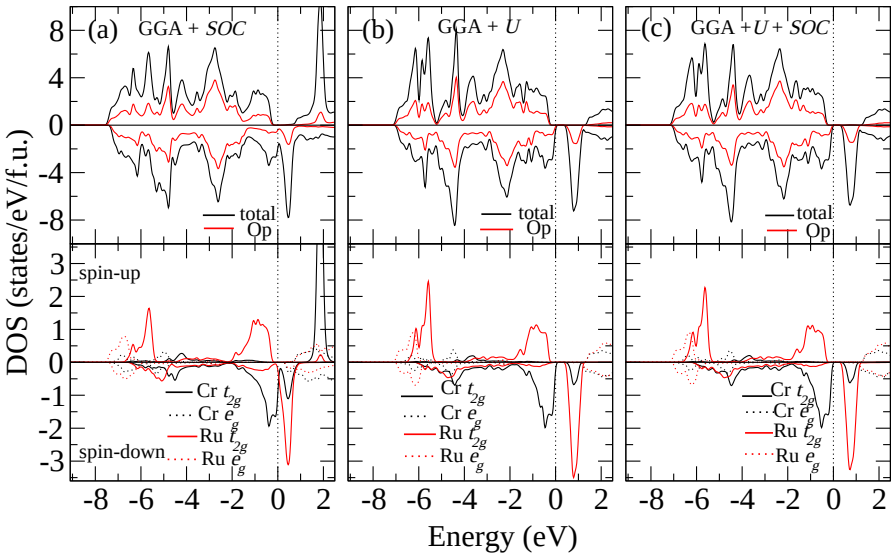

Figure 8: Total and orbital-decomposed density of states of Sr_2CrRuO_6 with $I4/mmm$ [111] structure, which $U = 3$ eV for Cr and 2 eV for Ru, and spin-orbital coupling (SOC).

ing magnetic interaction. In other words, $+U$ correction restores the structural-distorted Ba_2MoOsO_6 to be a HM-AFM. Compared to the correlation effects (several eV) seen in Figs. 6, 7 and 8, we can see that the SOC effect (several tenths eV) has less influence on the HM characteristics of the system. For example, in Sr_2MoOsO_6, with +SOC calculation,

there is no gap (Fig. 6(a)), however, with $+U$ calculation, there is a clear gap in spin-up channel (Fig. 6(b)). In Sr_2TcReO_6, with +SOC calculation, Fig. 7(a) shows a obviously HM character similar with Fig. 4(b), however, with $+U$ calculation, it becomes likely a Mott insulator (Fig. 7(b)). The spin-only picture is an idealization, SOC couples the two spin directions and thereby destroys the precise spin compensation, and in addition generates spin-induced orbital moments. Thus the half-metallicity is an idealization and what we can do is finding as close as possible a HM-AFM [31].

For Sr_2TcReO_6 in Fig. 7, due to electron-electron correlation effect, the Tc $t_{2g\uparrow}$ band is raised up and the Re $t_{2g\uparrow}$ band is lower down with respect to the Fermi-level. Therefore, the pseudogap appears in spin-up channel. The DOS of spin-up electrons falls to 0.17/0.06 (Table 2) following + U/+ U+SOC. Its HM characteristics has quenched and become a Mott-Insulator. For Sr_2CrRuO_6 in Fig. 8, the DOS of spin-down electrons falls to 0.44/0.05 (Table 2) following + U/+ U+SOC. Its HM characteristics also has quenched. In summary, correlation effect is important for HM characteristics since the stronger localization of d orbital electrons may break the conduction channel in HM.

4 Conclusions

We performed the self-consistent FLAPW electronic structure calculations to investigate all the possible 406 candidates of half-metallic (HM) antiferromagnet (AFM) in the [111] stacked structure $Sr_2BB'O_6$ where BB' pairs are any combination of 3d, 4d or 5d transition elements except for La. Sr can also be replaced by Ca or Ba whenever HM-AFM was found and similar calculation was repeated in order to probe more possibilities. As a result, We found that A_2MoOsO_6, A_2TcReO_6, A_2CrRuO_6, where A=Ca, Sr, Ba, with the [111] stacked structure are potential candidates of HM-AFM. In order to find the stable magnetic phase and structure in these three families of compounds, we further considered full structural optimization calculations by GGA method for these candidates in both [111] and [001] stacked structures with FM, AF-I and AF-II states. They are still HM-AFMs except for Ba_2MoOsO_6 which is NM. We also considered spin-orbit coupling (SOC) and correlation ($+U$) effects for these candidates by GGA+U and GGA+SOC methods. From Table 2 and DOS figures, we can see that the SOC effect has much less influence than the correlation effect on HM characteristics in these transition metal oxides. For A_2MoOsO_6, without $+U$ the HM feature of DOS is not obvious (pseudo gap for A= Ca, Sr and even NM feature for A= Ba). However, after considering $+U$, it is quite obvious by a HM-AFM. For A_2TcReO_6 and A_2CrRuO_6 (A=Ca, Sr, Ba), without $+U$, theirs HM features of DOS is obvious. However, after $+U$, they become nearly Mott-Insulators. Whether they are HM-AFMs or not need experimental confirmation. Nevertheless, considering the big difference of spin-up and spin-down band-gap near Fermi-level. A_2TcReO_6 and A_2CrRuO_6 (A=Ca, Sr, Ba) may still be suitable for the single-spin electron source providers. We hope that there will be further experimental evidence for these possible HM-AFMs in the future.

Acknowledgments

The authors gratefully acknowledge the generous financial supports received from the National Science Council (99B0320) and the National Center for Theoretical Sciences (NCTS), South Taiwan. The authors also wish to thank C. D. Hu for helpful discussions and the National Center for High-performance Computing (NCHC) of Taiwan for the use of their computers.

References

[1] R. A. de Groot, F. M. Müeller, P. G. van Engen, and K. H. J. Buschow, Phys. Rev. Lett. 50, 2024 (1983).
[2] J.-H. Park, E. Vescovo, H.-J. Kim, C. Kwon, R. Ramesh, and T. Venkatesan, Nature (London) 392, 794 (1998).
[3] K.-I. Kobayashi, T. Kimura, H. Sawada, K. Terakura, and Y. Tokura, Nature (London) 395, 677 (1998).
[4] W. E. Pickett and J. S. Moodera, Phys. Today 54, 39 (2001).
[5] H.-T. Jeng and G. Y. Guo, Phys. Rev. B 65, 094429 (2002).
[6] K. Schwarz, J. Phys. F: Met. Phys. 16, L211 (1986).
[7] W. E. Pickett and D. J. Singh, Phys. Rev. B 53, 1146 (1996).
[8] H.-T. Jeng and G. Y. Guo, Phys. Rev. B 67, 094438 (2003).
[9] M. S. Park, S. K. Kwon, S. J. Youn and B. I. Min, Phys. Rev. B 59, 10018 (1999).
[10] M. Shirai, T. Ogawa, I. Kitagawa and N. Suzuki, J. Magn. Magn. Mater. 177−181, 1383 (1998).
[11] J. H. Park, S. K. Kwon and B. I. Min, Physica B 281/282, 703 (2000).
[12] H. van Leuken and R. A. de Groot, Phys. Rev. Lett. 74, 1171 (1995).
[13] E. Salioglu, Phys. Rev. B 79, 100406 (2009).
[14] S. Wurmehl, H. C. Kandpal, G. H. Fecher, and C. Fecher, Jurnal Phys.: Condens. Matter, 18, 6171 (2006).
[15] I. Galanakis, K. Özdogan, E. Sasioglu, and B. Aktas, Phys. Rev. B 75, 172405 (2007).
[16] H. Luo, L. Ma, Z. Zhu, G. Wu, H. Liu, J. Qu and Y. Li, Physica B 403, 1797 (2008).
[17] Jürgen, B. Balke, G. H. Fecher and C. Felser, Phys. Rev. B 77, 054406 (2008).
[18] M. S. Park, S. K. Kwon, and B. I. Min, Phys. Rev. B 64, 100403(R) (2001).
[19] M. NaKao, Phys. Rev. B 83, 214404 (2011).
[20] M. NaKao, Phys. Rev. B 74, 172404 (2006).
[21] M. NaKao, Phys. Rev. B 77, 134414 (2008).
[22] J. H. Park, S. K. Kwon, and B. I. Min, Phys. Rev. B 65, 174401 (2002).
[23] D. Ködderitzsch, W. Hergert, Z. Szotek and W. M. Temmerman, Phys. Rev. B 68, 125114 (2003).
[24] I. Galanakis, K. Özdogan, E. Sasioglu, and B. Aktas, Phys. Rev. B 75, 092407 (2007).
[25] H. Akai and M. Ogura, Phys. Rev. Lett. 97, 026401 (2006).
[26] L. Bergqvist and P. H. Dederichs, Jurnal Phys.: Condens. Matter, 19, 216220 (2007).
[27] W. E. Pickett, Phys. Rev. B 57, 10613 (1998).
[28] Y. K. Wang and G. Y. Guo, Phys. Rev. B 73, 064424 (2006).
[29] S. H. Chen, Z. R. Xiao, Y. P. Liu and Y. K. Wang, J. Appl. Phys. 137018JAP (2010).
[30] Y. K. Wang, P. H. Lee and G. Y. Guo, Phys. Rev. B 80, 224418 (2009).
[31] V. Pardo and W. E. Pickett, Phys. Rev. B 80, 054415 (2009).

[32] K. W. Lee and W. E. Pickett, Phys. Rev. B 77, 115101 (2008).
[33] E. Sasioglu, C. Friedrich and S. Blügel, Phys. Rev. B 83, 121101 (2011).
[34] P. E. Blöchl, Phys. Rev. B 50, 17953 (1994); G. Kresse and D. Joubert, Phys. Rev. B 59, 1758 (1999).
[35] G. Kresse, and J. Hafner, Phys. Rev. B 48, 13115 (1993); G. Kresse and J. Furthmüller, Comput. Mater. Sci. 6, 15 (1996); Phys. Rev. B 54, 11169 (1996).
[36] P. Blaha, K. Schwarz, G. K. H. Madsen, D. Kvasnicka, and J. Luitz, wien2K, An Augmented Plane Wave Local Orbitals Program for Calculating Crystal Properties Techn. University Wien, Austria, (2005).
[37] O. K. Andersen, Phys. Rev. B 12, 3060, (1975).
[38] D. D. Koelling and G. O. Arbman, J. Phys. F: Met. Phys. 5, 2041 (1975).
[39] P. E. Blochl, O. Jepsen, and O. K. Andersen, Phys. Rev. B 49, 16223 (1994).
[40] V. I. Anisimov, I. V. Solovyev, M. A. Korotin, M. T. Czyzyk, and G. A. Sawatzky, Phys. Rev. B 48, 16929 (1993).
[41] V. I. Anisimov, F. Aryasetiawan, and A.I. Lichtenstein, J. Phys.: Condens. Matter 9, 767 (1997).
[42] I. V. Solovyev, P. H. Dederichs and V. I. Anisimov, Phys. Rev. B 50, 16861 (1994).
[43] C. Zener, Phys. Rev. 82, 403 (1951).
[44] I. V. Solovyev and K. Terakura, Phys. Rev. Lett 82, 2959 (1999).
[45] I. V. Solovyev and K. Terakura, in Electronic Structure and Magnetism of Complex Materials, edited by D. J. Singh and D. A. Papaconstantopoulos (Springer-Verlag, Berlin, 2003).
[46] H.-T. Jeng and G. Y. Guo, Phys. Rev. B 67, 094438 (2003).
[47] H. Wu, Phys. Rev. B 64, 125126 (2001).